

Research Article

UNDERSTANDING STRUCTURAL BASIS FOR REDOX REGULATION OF PEROXIREDOXIN 6 USING *IN SILICO* APPROACH

Rimpy Kaur Chowhan¹, Upendra Bhele¹, Hamidur Rahaman², and Laishram Rajendrakumar Singh^{1,*}

¹Dr. B.R. Ambedkar Center for Biomedical Research, University of Delhi, Delhi 110007, India; ²Department of Biotechnology, Manipur University, Imphal, Manipur-795003, India

Abstract: Peroxiredoxin6 (Prdx6) belongs to a family of antioxidant enzymes called peroxiredoxins which rescue cells from oxidative stress by hydrolysing peroxides and peroxidised macromolecules. Prdx's active site always constitutes a Cys residue whose redox status regulates peroxidase function such that the enzyme with oxidised Cys is inactive and reduced Cys is active. However, our knowledge regarding human Prdx6 structure is limited only to its oxidised form. This limits our understanding of the conformational changes underlying redox regulation of its peroxidase activity. In the present study, we have used MD simulations to model and analyse reduced human Prdx6 (rPrdx6). Comparison of our simulated structure of rPrdx6 with that of the oxidised crystal structure (oPrdx6) revealed that Prdx6 induces redox-mediated conformational alterations at both tertiary and secondary structure level to regulate its peroxidase function. Since, other Prdx family members also alter their conformation due to change in oxidation status, it appears that such redox coupled structural changes are intrinsic catalytic property of Prdx family.

Keywords: Peroxiredoxin 6; structure; redox regulation; MD simulation; GROMACS

Note : Coloured Figures and Supplementary Information available on Journal Website in "Archives" Section

Introduction

Oxidative stress is one of the most common and deleterious toxic insults endured by cells during diseased conditions. To counter this, cells have a robust defence system comprising antioxidants like glutathione, thioredoxin, ascorbate, etc. and antioxidative enzymes including glutathione peroxidase, catalase, superoxide dismutase and peroxiredoxins (Prdx). Prdx family comprises of ubiquitously expressed highly conserved non-heme peroxidases that have ability to detoxify peroxides and peroxidised macromolecules by hydrolysing

them with the help of active cysteine residues and an electron donor which is usually thioredoxin. The exception is Prdx6 which instead uses glutathione and ascorbate as physiological reductant (Monteiro *et al.*, 2007; Sharapov *et al.*, 2014). In fact, Prdx6 has many exceptional properties that makes it unique among its fellow family members, for example, in addition to glutathione peroxidase activity it also exhibits an additional moonlighting function of calcium independent phospholipase A2 (aiPLa2) activity for hydrolysis of fatty acyl ester bond of glycerophospholipid to form free lysophospholipids and fatty acids within the lysosome (Fisher, 2011). Prdx6 dual activity is modulated by various factors such as change in pH, post-translational modifications, interaction with pi class glutathione-S-transferase (Chatterjee *et al.*, 2011; Fisher, 2011; Kim *et al.*, 2008; Manevich *et al.*, 2009; Rahaman *et*

Corresponding Author: Laishram R. Singh

E-mail: lairksingh@gmail.com

Received: August 01, 2017

Accepted: October 21, 2017

Published: October 23, 2017

al., 2012; Ralat *et al.*, 2006; Wu *et al.*, 2006; Wu *et al.*, 2009). For instance, at neutral pH, Prdx6 behaves as a peroxidase while in acidic pH its aiPLA2 activity is maximal (Manevich *et al.*, 2009). Phosphorylation on the other hand, allows Prdx6 to function as aiPLA2 at cytosolic pH as well (Wu *et al.*, 2009).

Prdx6 has earlier been known to exhibit redox regulated catalytic activity. Since, changes in the redox status tends to affect structure or oligomeric status of enzymes, we were interested to understand the underlying conformational modifications due to change in oxidation status of Prdx6. To date, the knowledge regarding Prdx6 structure is limited to the x-ray crystallographic structure of oxidised Prdx6 (oPrdx6) (PDB ID: 1prx) (Choi *et al.*, 1998). Moreover, this crystal structure also has few shortcomings- (i) the wwPDB X-ray structure validation server has described the quality of 1prx structure to be below average (for detailed report, see http://ftp.wwpdb.org/pub/pdb/validation_reports/pr1prx/1prx_full_validation.pdf), (ii) there is a discrepancy within the X-ray structure and reference sequence (gene ID: 9588) that the cysteine residue at 91 position is mutated to serine residue, (iii) a N-terminal residue (residue 1) and five residues in a solvent exposed loop between helix α 4 and strand β 6 (residues 122-126) are missing in the crystal structure (Choi *et al.*, 1998). It may be noted that since Cys47 is reduced in the active Prdx6, the crystal structure with oxidised Cys47 primarily represents some catalytic intermediate. It is not advisable to solely use oPrdx6 structure to understand the underlying structure function interplay of peroxidase catalytic cycle (Choi *et al.*, 1998; Peshenko *et al.*, 2001).

It is known that deficiency or inactivation of Prdx6's peroxidase activity under diseased condition renders cellular defence mechanism ineffective against elevated oxidative stress (Hirota *et al.*, 2010; Manevich *et al.*, 2005; Wang *et al.*, 2003). Prdx6 plays crucial role in multiple diseases including emphysema, asthma, chronic lung injury, cataract, type 2 diabetes, ischemia, carcinogenesis, Prion disease, Alzheimer's disease, Parkinson's disease and metastasis of cancerous cells (Hasanova *et al.*, 2009; Li *et al.*, 2012; Nagy *et al.*, 2006; Nicolussi *et al.*, 2014; Pacifici *et al.*, 2014; Park *et al.*, 2016; Wang *et al.*, 2008; Yun *et al.*, 2015; Yun *et al.*, 2013). However, lack of structural insights limits our understanding of its catalytic activity, functional allosteric and regulatory mechanisms of Prdx6,

making it difficult to understand Prdx6's involvement in etiology of these diseases.

Other than the general nature of Prdx's to alter their conformation with change in their redox status (Barranco-Medina *et al.*, 2009), our hypothesis that rPrdx6 is conformationally different from oxidised protein also arises from the fact that the crystal structure of oPrdx6 fails to explain certain observations made during biochemical analysis of the protein which would have been more lucid with the knowledge of rPrdx6 structure (Chatterjee *et al.*, 2011; Wu *et al.*, 2009). These discrepancies are later discussed in detail within the results and discussion. Since, recombinant production at high concentrations and growing crystals for Wt human rPrdx6 is challenging, to verify our hypothesis and unambiguously depict protein structure we have modelled and simulated the structure of rPrdx6. This simulated structure is appropriate to explain most of the biochemical and functional insights and also provides platform for better understanding of enzyme's structure-function correlation using *in silico* approaches.

Materials and Methods

Generating 3D model of reduced Prdx6 - The data on the human PRDX6 gene (Gene ID: 9588) and related protein sequence (Uniprot ID: P30041) was collected from gene database of National Center for Biological Information (<https://www.ncbi.nlm.nih.gov/gene/9588>) and UniProt database (<http://www.uniprot.org/uniprot/P30041>), respectively. The 3D structure of Wt rPrdx6 was modelled using I-TASSER online server (Zhang, 2008). The raw amino acid sequence of Prdx6 was uploaded in FASTA format to I-TASSER server, which then used crystal structure of C91S mutant human Prdx6 (oPrdx6) (PDB ID: 1prxA) (Choi *et al.*, 1998) and C47S mutant Arenicola Prdx6 (PDB ID: 2v2gA) (Smeets *et al.*, 2008) as templates to provide protein model in PDB format. Structure validation parameters (measured by I-TASSER); confidence score 4 1.59 and TM-score 4 0.94 \pm 0.5, indicated the structure model to be of good quality (Yang *et al.*, 2015). The primary sequence of Wt rPrdx6 model structure thus generated had following changes from that of crystal structure- (i) Cys sulfenic acid (Cys-SOH) at 47th position was replaced with reduced Cys residue (Cys-SH), (ii) Ser91 was mutated to Cys residue, and (iii) the N-terminal residue (residue 1) and five residues in a solvent exposed loop between helix α 4 and strand β 6 (residues 122-126) that were missing in crystal

structure model were introduced. The structures were visualized using Pymol (Lill *et al.*, 2011).

MD simulation and structure validation- MD simulation was performed using GROMACS 4.6.5 software package (Hess *et al.*, 2008) running on a Tyrone Camarero SS300TR-34 machine with Intel Xeon E5-2630v3 processor, 32 GB RAM and running Fedora 21 package. The algorithm used was CHARMM27 all-atom force field. Structure of modelled rPrdx6 protein was used as starting point for MD simulations. The topology parameters of protein were created by using the Gromacs program. The protein was immersed in a cubic box of simple point charge (SPC) water molecules. At physiological pH the structure was found to be negatively charged; so two Na⁺ counter-ions were added by replacing water molecules to make the simulation system electrically neutral. To relieve discordant contacts, energy minimization was done using the steepest descent method of maximum 50000 steps until maximum force < 1000.0 KJ/mol/nm is reached. For system equilibration, solute was subjected to the position-restrained dynamics simulation (NVT and NPT) at 300K temperature for 1000ps. Finally, the whole system was subjected to MD production run at 300K temperature and 1 bar pressure for 50000ps. For analysis, the atom coordinates were recorded at every 10ps during the MD simulation. The rPrdx6 model obtained at the end of simulation was used for further analysis and its quality was verified using PROSA, ERRAT, Verify-3D and RAMPAGE server (Bowie *et al.*, 1991; Colovos *et al.*, 1993; Lovell *et al.*, 2003; Wiederstein *et al.*, 2007). However, structure visualization was performed by the Swiss PDB viewer and PyMol (Guex *et al.*, 1997; Lill *et al.*, 2011).

Analysis of MD simulation trajectory - The trajectory files were computed using g_rmsd, g_rmsf, g_sasa and g_gyrate to obtain RMSD, RMSF, SASA (solvent accessible surface area) and Rg plot of human rPrdx6 simulation was used to visualize these graphical profiles.

Secondary structure and solvent exposure estimation - Secondary structure estimation of the protein was done using 2Struc server (Klose *et al.*, 2010) which defined secondary structure of proteins by DSSP method. DSSP is a well-established protocol used worldwide for identifying protein's secondary structure using pattern-detection procedure of hydrogen-bonds and geometrical characteristics

extricated from x-ray coordinates. 2Struc server asks for PDB structure files as input to describe secondary structure as the percentage share of alpha helices, beta sheets, and others.

Solvent exposure or SASA of amino acids as per their location in the protein model was evaluated using ASAView server (Ahmad *et al.*, 2004). PDB structure files with protein chain id was provided as input file, and a graphical result was obtained in the form of a spiral plot of amino acids where radius of each amino acid sphere is proportional to the SASA of that amino acid.

Results and Discussion

It is known that Prdx6 is not only required for combating cellular oxidative stress but also is an important therapeutic candidate for large number of human diseases including, neurodegeneration, diabetes, respiratory diseases, cancer, etc (Hasanova *et al.*, 2009; Li *et al.*, 2012; Nagy *et al.*, 2006; Nicolussi *et al.*, 2014; Pacifici *et al.*, 2014; Park *et al.*, 2016; Wang *et al.*, 2008; Yun *et al.*, 2015; Yun *et al.*, 2013). However, the complete disease aetiologies by which Prdx6 influence cellular system and homeostasis in these diseases could not be unfolded in detail due to the lack of knowledge on Prdx6's structural allosteric and structure-function relationships. Additionally, as described earlier, the absence of an appropriate crystal structure of Wt rPrdx6, necessitated the generation of an *in silico* based MD-simulated structure for better understanding of underlying structural interplay during Prdx6 mediated biochemical reactions, its catalytic activity, functional allosteric and regulatory mechanisms.

We constructed 3D model of wild type human rPrdx6 using crystal structure of oxidised C91S Prdx6 (1PrxA) as a template since 1PrxA has highest (97%) similar identity to sequence of Wt human Prdx6. The structural modifications introduced in the template structure included - (i) altering redox status of oxidised Cys47 to reduced state and (ii) replacing Ser91 by Cys91. Interestingly, Ryu and co-workers have revealed using crystal structure of oPrdx6 (1Prx) that to be catalytically active (i.e. reduced state), rPrdx6 has to be essentially monomer because in the dimeric form P191 gets into the catalytic pocket, narrows the passage for substrate entry and inhibits its peroxidase activity (Choi *et al.*, 1998). It is assumed that Prdx6 undergoes dimer-monomer transition for carrying

out its peroxidase activity, where rPrdx6 monomer gets self-oxidised to reduce the peroxidised substrates, and oPrdx6 then associate together to achieve a catalytic intermediate dimeric conformation which is also believed to be the cellular storage form of the protein. Therefore, to achieve a structure as close as possible to the catalytically active form of native Prdx6, we have modelled rPrdx6 structure as a monomer.

Further structural refinement was done by carrying out energy minimization and structure equilibration using MD simulation. This also helped to analyse the stability and dynamics of rPrdx6 by monitoring its structural behaviour during the course of entire simulation run. The RMSD (root mean square deviation) plot (see Figure 1A) describing the measure of average distance between the backbone atoms of various protein conformations achieved during the simulation and the initial relaxed modelled protein structure showed Prdx6 to have various conformational sub-populations in its folding funnel. RMSD first increased to 0.2nm in the initial 1000ps, then took a steep escalation to 0.54nm around 10000ps, and finally equilibrated after 22000ps with RMSD \sim 0.39nm. The different conformations generated during simulation run were also analysed using radius of gyration (R_g) and SASA profile (see Figure 1B and 1C). While, R_g depicts the overall packing of protein conformers formed during the simulation, SASA describes about the area of protein that is exposed to interact with the solvent. Both R_g and SASA profile seems to be relatively constant throughout the course of simulation with R_g of around 2.02–2.1 nm and SASA of 138–145 nm 2 , indicating that whatsoever conformational changes that have happened during structural refinement have not largely affected the overall shape of rPrdx6 during the course of simulation.

RMSF (root mean square fluctuation) provides a good description of protein flexibility on a residue-by-residue basis by recording the positional fluctuation of each amino acid from its time-averaged position of each carbon atom. Unlike other descriptors of backbone motions like crystallographic B-factors, RMSF can be consistently used to evaluate flexibility within various structural regions as it is not affected by additional factors besides internal fluctuations (Hunenberger *et al.*, 1995). As seen in Figure 2, RMSF analysis of rPrdx6 simulation revealed C-terminal domain (residues 175–224) (atoms 2760–3566) to be the most flexible

region of the structure during the entire course of simulation. Additionally, other flexible regions with RMSF greater than 0.4 nm, observed were residues 92–94 (atoms 1404–1432), residues 121–122 (atoms 1869–1917), and residues 139–140 (atoms 2152–2170). The enhanced flexibility of these residues compared to other amino acids could be attributed to their localization within loops which inherently have high entropy. Flexibility in these regions could also be seen in pictorial snapshots of rPrdx6 conformations taken at various simulation time scales (See Figure 3) especially in the C-terminal domain where secondary structure alterations are very apparent.

Since there was insignificant variation in the RMSD (of around 0.1nm) of the conformations achieved after the structural equilibration, we have used the final structure obtained at the end of the simulation for further studies. To validate this simulated structure of human rPrdx6, four different commonly used structural analysis and verification servers were used including RAMPAGE, PROSA, ERRAT and Verify-3D (Bowie *et al.*, 1991; Colovos *et al.*, 1993; Lovell *et al.*, 2003; Wiederstein *et al.*, 2007). Web server RAMPAGE (Lovell *et al.*, 2003) (Supplementary FigureS1) aided in visualizing the localization of rPrdx6's residues within the Ramachandran plot in accordance with the dihedral angles associated with their backbone carbon atom. We found approximately 94% residues to fall in the favourable region and none in the disallowed region. Results obtained from PROSA (Wiederstein *et al.*, 2007) (See supplementary FigureS2) revealed the quality of simulated rPrdx6 structure to be equivalent to that of structures obtained using NMR spectroscopy. These results are quantitated in the terms of z-score, which is calculated for a query PDB file and then compared with the z-scores pre-calculated for structures deposited in PDB databases from different sources including X-Ray and NMR. ERRAT (Colovos *et al.*, 1993) is another verification server that uses the statistics of highly refined structures to analyse non-bonded interactions between various atoms, and provides plot for error function values versus position of a 9-residue sliding window. This statistical analysis also showed simulated rPrdx6 structure to be of good quality with overall quality factor of 94.53. Our simulated model of Wt human rPrdx6 also passed the quality assessment done by VERIFY-3D (Bowie *et al.*, 1991) server with 88.69% residues in the 3D atomic model showing compatibility with

the 1D amino acid sequence based secondary structure allocation. Supplementary Table S1 summarizes the quality prediction scores of each server for simulated rPrdx6 structure. The well-defined valid scores from each of the analytical servers led us to believe that our simulated structure is of excellent quality and could be used for further structural analysis.

To comprehend the redox regulation of Prdx6 conformation, we first compared secondary structure of oPrdx6 (PDB Id: 1Prx) (Choi *et al.*, 1998) with rPrdx6 using 2struc server's DSSP based algorithm (Klose *et al.*, 2010). We found overall 4% and 20% reduced alpha helical and beta sheet content in rPrdx6, respectively (Table 1). To further identify the regions corresponding to these secondary structure alterations, we superimposed images of oPrdx6 (1prx) and rPrdx6 structure (our simulated structure) (Figure 4). At the outset, we observed that most loops in the oPrdx6 are more solvent exposed than that of our simulated structure indicating oxidised protein to have relatively more flexible conformation than its native counterpart. This is quite understandable because the oxidised protein is a catalytic intermediate and need to interact with other binding partners (e.g., Glutathione-S-transferase) to complete the redox cycle and has to be more flexible (Kang *et al.*, 1998; Ralat *et al.*, 2006). After detailed analysis, we found alleviated alpha helical levels of rPrdx6 corresponded to the shortening of helix $\alpha 5$ (residue 171-173) (Figure 5). We also noticed a slight restoration of helical twist at residue 56-58 in helix $\alpha 2$ within simulated structure (Figure 6). We believe that a small change in the helix $\alpha 2$ is responsible for reduced and oxidised protein to exist in active and inactive conformations respectively because the restoration of twists within the alpha helical region $\alpha 2$ at residues 56-58 of rPrdx6 will help to lower the pKa of thiol at active site making the enzyme affinity with substrates higher. It is known that a

Table 1
Secondary structure analysis. Percentage content of secondary structure components in oxidised (crystal structure) and of human reduced Prdx6 (our simulated structure) as determined by 2Struc server

	Oxidised Prdx6	Reduced Prdx6
Alpha helix	29%	27.7%
Beta strand	20.5%	16.5%
Others	50.4%	55.8%

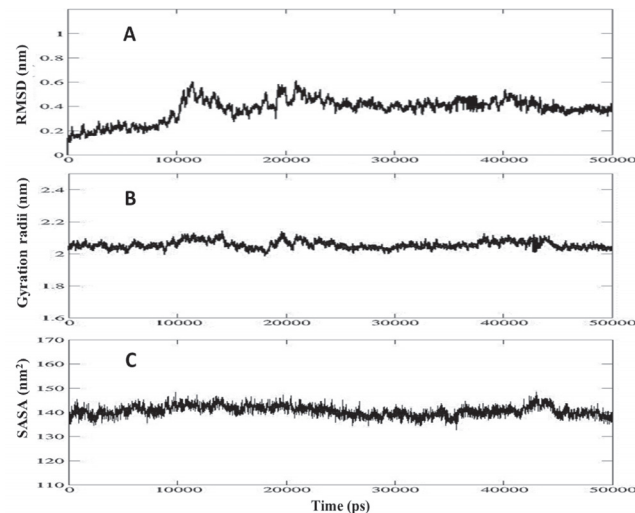


Figure 1: Structural model refinement analysis of Wt human reduced Prdx6's simulated structure. A) Root mean square deviation (RMSD), B) the radius of gyration, and C) Solvent accessible surface area (SASA) profile

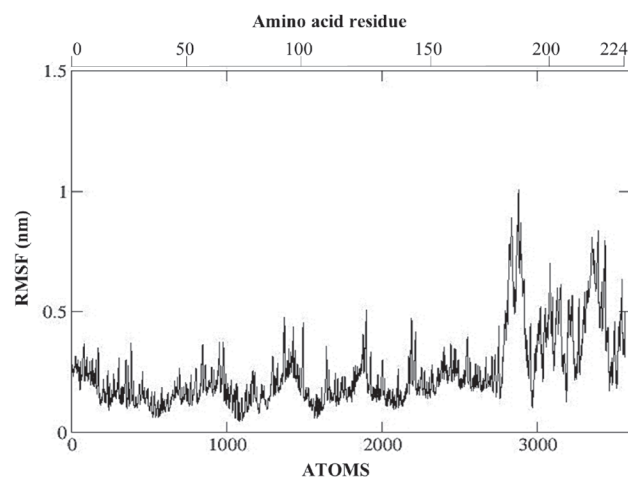


Figure 2: Root mean square fluctuation (RMSF) profile of Wt human reduced Prdx6

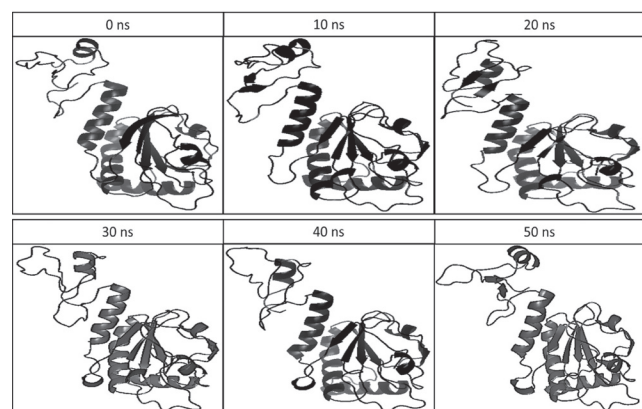


Figure 3: Snapshots of human Prdx6 models taken at different time scales during MD simulation

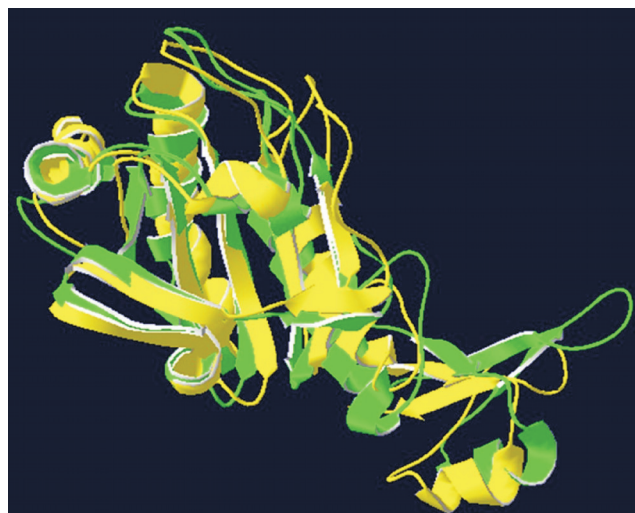


Figure 4: Superimposed images of crystal structure of oxidised Prdx6 (green) with model of reduced Prdx6 (yellow)

favourable interaction of thiolate anion with the peptide dipoles of alpha helix pointing towards the catalytic site has the ability to stabilize the thiolate and reduce its pKa by 1.5 to 2.1 pKa units (Carvalho *et al.*, 2006; Kortemme *et al.*, 1995). On the other hand, oxidized protein becomes inactive due to at least two reasons: (i) lack of peptide dipole orientation toward the catalytic site, and (ii) narrowing of the passage of substrate entry due to P191 entry into the catalytic site.

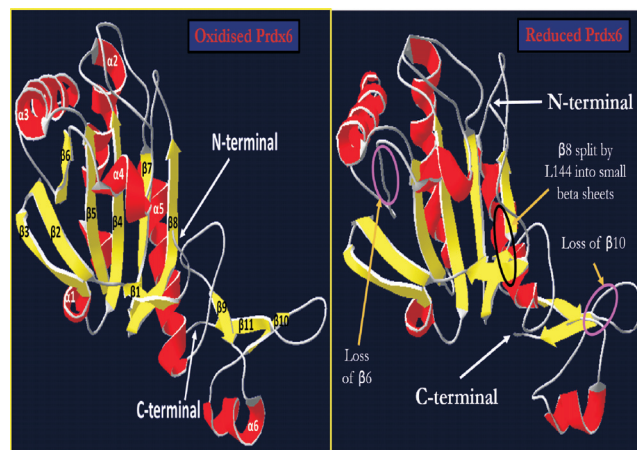


Figure 5: Secondary structure differences between oxidised (crystal structure 1Prx) and reduced (our simulated model) human Prdx6. Beta sheets and alpha helices are coloured yellow and red respectively

Furthermore, the underlying reason for 20% reduction in total beta content of rPrdx6 was realised to be (i) loss of β6 and β10 strands, and (ii) splitting of β8 into two smaller strands due to introduction of a random coil by residue L144 (Figure 5). Moreover, surface accessible solvent exposure analysis of oPrdx6 and rPrdx6 on residue-by-residue basis revealed rearrangements of some residue's solvent accessibility. For instance,

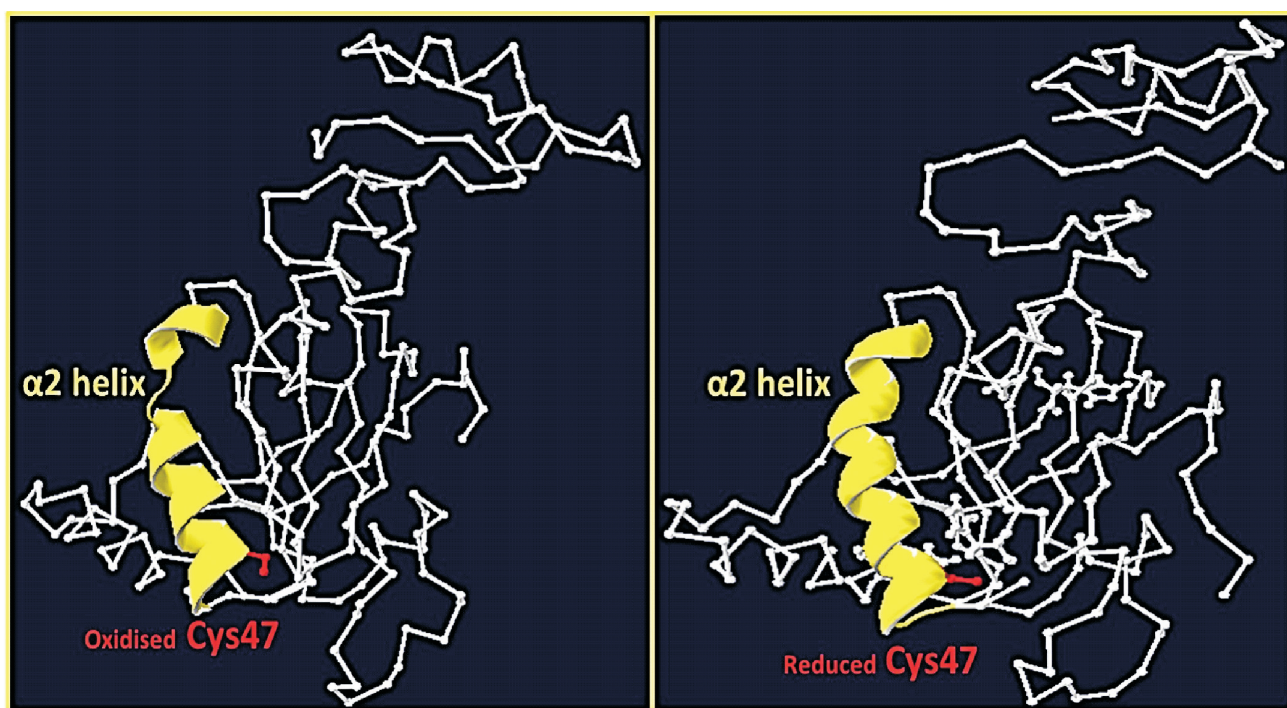


Figure 6: Human Prdx's oxidised structure (right panel) and reduced structure (left panel) with active site Cysteine 47 residue (red) and the alpha-helix (yellow) pointing towards it

enzyme's T177 residue was buried in the core region of the inactive oPrdx6 dimer with 0% solvent contact but was exposed in rPrdx6 (Figure 7). Interestingly, T177 is an important regulatory site whose phosphorylation allows Prdx6 to function as aiPla2 in cytosolic pH (Chatterjee *et al.*, 2011; Rahaman *et al.*, 2012; Wu *et al.*, 2009) and its presence in core region of oPrdx6 fails to explain the feasibility of post-translational modification of Prdx6's T177 residue within cytosol. However, presence of T177 as a solvent exposed residue in rPrdx6 clearly clarifies the operability of this phenomenon in cellular milieu. Thus, our simulated structure not only helps to explain the structural alterations between oxidised and reduced form of Prdx6 but also gives insight on the underlying

structural interplay during this key biochemical event. Remarkably, we noted that although there exists many conformational differences between rPrdx6 and oPrdx6, they do not much affect the positioning and arrangement of its major catalytic domain, the thioredoxin fold region comprising of a beta core ($\beta 4$, $\beta 5$, $\beta 7$ and $\beta 8$) surrounded by 3 alpha helices ($\alpha 2$, $\alpha 4$ and $\alpha 5$) (Sharapov *et al.*, 2014). Taken together, it seems that change in redox status of Prdx6 doesn't disturb its active site fold or ability to be a peroxidase but alters the conformation of non-catalytic domains such that the rPrdx6 is more prone to interact with substrate while oPrdx6 is more flexible, a characteristic common of catalytic intermediates. Interestingly, proteins like Prdx5, tyrosine phosphatase 1B and Jun-Fos are also

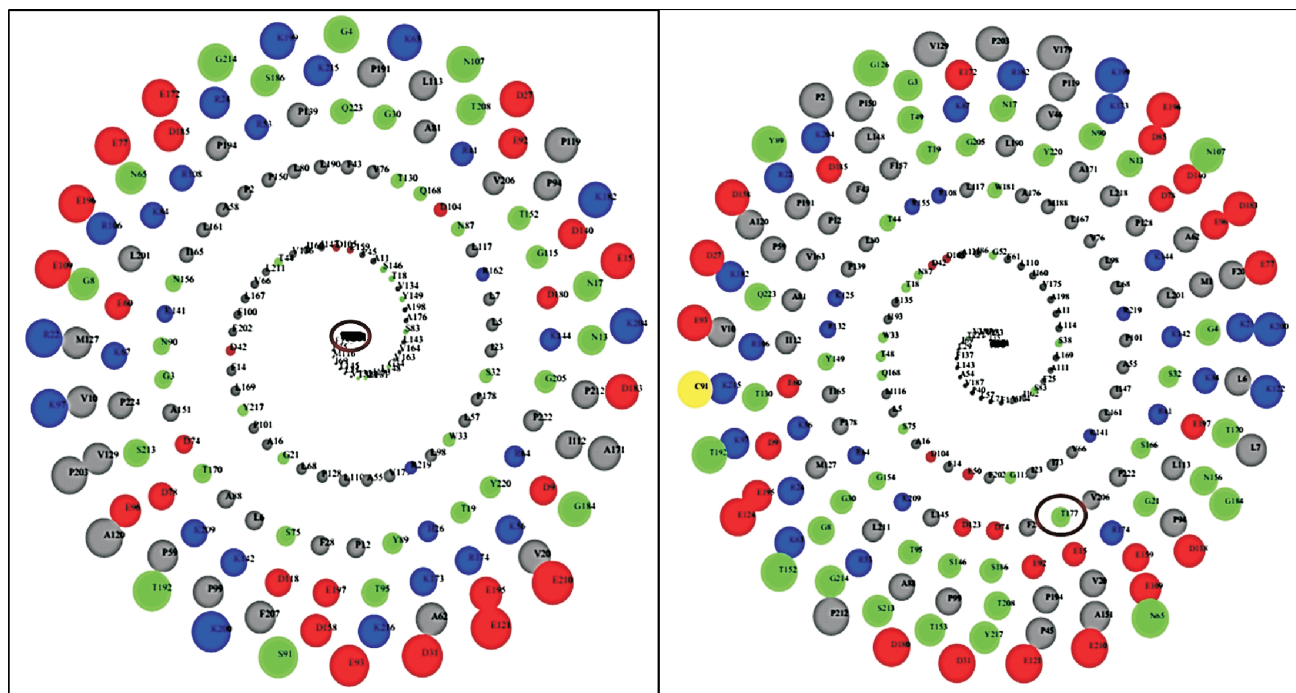


Figure 7: Solvent exposed surface area (SASA) analysis of each amino acid residues in crystal structure (left panel) and reduced Prdx6 structure (right panel). As seen in left panel, T177 residue (highlighted by circling) is in the centre of the spiral SASA plot which represents buried core region of the oxidised inactive Prdx6 while in the case of reduced active Prdx6 (right panel) T177 is exposed

Supplementary Table S1. Structure model validation. Scores provided by RAMPAGE, PROSA, Verify-3D, and ERRAT server after estimating the quality of reduced human Prdx6

RAMPAGE			PROSA	Verify-3D	ERRAT
no. of residues in :					
Favored region	Allowed region	Outlier region	Z-score	residues with averaged 3D-1D score >= 0.2	Overall quality factor
93.90%	5.20%	0.90%	-7.76	88.69%	94.53

known to regulate their physiological functions in a similar fashion. (Abate *et al.*, 1990; Declercq *et al.*, 2001; Evrard *et al.*, 2004; Salmeen *et al.*, 2003). Prdx5, for example in its active state exist as a monomer, while oxidation of its Cys residue stimulates dimerization rendering Prdx5 inactive due to masking of its oxidation site (Evrard *et al.*, 2004). There have been other reports as well where few Prdx family members has been seen to alter their conformation drastically and control their peroxidase activity by changing oxidation status of active site Cys residue (Barranco-Medina *et al.*, 2009). Taken together, it appears that such redox coupled structural changes are intrinsic catalytic property of Prdx family.

Conclusion

We have modelled and simulated the structure of rPrdx6. The structure thus generated is able to explain the important biochemical events including post-translation modification of Prdx6. Based on the systematic comparison between rPrdx6 and oPrdx6, we concluded that Prdx6 utilizes redox-mediated conformational alterations to regulate its function. For this, it uses alteration of peptide dipole of helix α 2 and orients residues such that the catalytic domain is unaffected but the entry of substrate near the active site is manoeuvred in both states, thereby allowing reduced and oxidised protein to exist in active and inactive conformation respectively.

Acknowledgement

This work is supported by the grant provided by the Department of Biotechnology (Ref No.: BT/359/NE/TBP/2012). Authors also acknowledge Council of Scientific and Industrial Research for the financial assistance provided in the form of research fellowship of Rimpay Kaur Chowhan (File No.: 09/045(1245)/2012-EMR-1) and DBT-Bioinformatics Infrastructure Facility at Dr. B. R. Ambedkar Center for Biomedical Research, Delhi University for providing infrastructure facility. The funders had no role in decision to publish, or preparation of the manuscript.

Conflict of interest

The author(s) declare no competing interests.

Abbreviations

aiPLA₂, calcium independent phospholipase A2; CAPRI, Critical assessment of prediction of interactions; DSSP, Defined secondary structure of proteins; GROMACS, GROningen MAchine for Chemical Simulations, Prdx6, Peroxiredoxin 6; π GST, pi class glutathione-S-transferase;

Rg, Radius of gyration; RMSD, Root mean square deviation; RMSF, Root mean square fluctuation; SASA, Solvent accessible surface area.

References

- Abate, C., Patel, L., Rauscher, F. J. D. and Curran, T. (1990). Redox regulation of fos and jun DNA-binding activity in vitro. *Science* 249, 1157-1161.
- Ahmad, S., Gromiha, M., Fawareh, H. and Sarai, A. (2004). ASAView: database and tool for solvent accessibility representation in proteins. *BMC Bioinformatics* 5, 51.
- Barranco-Medina, S., Lázaro, J.-J. and Dietz, K.-J. (2009). The oligomeric conformation of peroxiredoxins links redox state to function. *FEBS Lett* 583, 1809-1816.
- Bowie, J. U., Luthy, R. and Eisenberg, D. (1991). A method to identify protein sequences that fold into a known three-dimensional structure. *Science* 253, 164-170.
- Carvalho, A. P., Fernandes, P. A. and Ramos, M. J. (2006). Similarities and differences in the thioredoxin superfamily. *Prog Biophys Mol Biol* 91, 229-248.
- Chatterjee, S., Feinstein, S. I., Dodia, C., Sorokina, E., Lien, Y.-C., Nguyen, S., Debolt, K., Speicher, D. and Fisher, A. B. (2011). Peroxiredoxin 6 phosphorylation and subsequent phospholipase A2 activity are required for agonist-mediated activation of NADPH oxidase in mouse pulmonary microvascular endothelium and alveolar macrophages. *J Biol Chem* 286, 11696-11706.
- Choi, H. J., Kang, S. W., Yang, C. H., Rhee, S. G. and Ryu, S. E. (1998). Crystal structure of a novel human peroxidase enzyme at 2.0 Å resolution. *Nat. Struct. Mol. Biol.* 5, 400-406.
- Colovos, C. and Yeates, T. O. (1993). Verification of protein structures: patterns of nonbonded atomic interactions. *Protein Sci.* 2, 1511-1519.
- Declercq, J. P., Evrard, C., Clippe, A., Vander Stricht, D., Bernard, A. and Knoops, B. (2001). Crystal structure of human peroxiredoxin 5, a novel type of mammalian peroxiredoxin at 1.5 Å resolution. *J Mol Biol* 311, 751-759.
- Evrard, C., Capron, A., Marchand, C. c., Clippe, A., Wattiez, R., Soumillion, P., Knoops, B. and Declercq, J.-P. (2004). Crystal structure of a dimeric oxidized form of human peroxiredoxin 5. *J Mol Biol* 337, 1079-1090.
- Fisher, A. B. (2011). Peroxiredoxin 6: a bifunctional enzyme with glutathione peroxidase and phospholipase A2 activities. *Antioxid Redox Signal* 15, 831-844.
- Guex, N. and Peitsch, M. C. (1997). SWISS-MODEL and the Swiss-Pdb Viewer: an environment for comparative protein modeling. *Electrophoresis* 18, 2714-2723.
- Hasanova, N., Kubo, E., Kumamoto, Y., Takamura, Y. and Akagi, Y. (2009). Age-related cataracts and Prdx6: correlation between severity of lens opacity, age and the level of Prdx 6 expression. *Br J Ophthalmol* 93, 1081-1084.
- Hess, B., Kutzner, C., Van Der Spoel, D. and Lindahl, E. (2008). GROMACS 4: algorithms for highly efficient,

- load-balanced, and scalable molecular simulation. *J. Chem. Theory Comput.* 4, 435-447.
- Hirota, Y., Acar, N., Tranguch, S., Burnum, K. E., Xie, H., Kodama, A., Osuga, Y., Ustunel, I., Friedman, D. B. and Caprioli, R. M. (2010). Uterine FK506-binding protein 52 (FKBP52) & peroxiredoxin-6 (PRDX6) signaling protects pregnancy from overt oxidative stress. *Proc. Natl. Acad. Sci. U.S.A.* 107, 15577-15582.
- Hunenberger, P. H., Mark, A. E. and Van Gunsteren, W. F. (1995). Fluctuation and cross-correlation analysis of protein motions observed in nanosecond molecular dynamics simulations. *J Mol Biol* 252, 492-503.
- Kang, S. W., Baines, I. C. and Rhee, S. G. (1998). Characterization of a mammalian peroxiredoxin that contains one conserved cysteine. *J Biol Chem* 273, 6303-6311.
- Kim, S. Y., Jo, H.-Y., Kim, M. H., Cha, Y.-y., Choi, S. W., Shim, J.-H., Kim, T. J. and Lee, K.-Y. (2008). H₂O₂-dependent hyperoxidation of peroxiredoxin 6 (Prdx6) plays a role in cellular toxicity via up-regulation of iPLA2 activity. *J Biol Chem* 283, 33563-33568.
- Klose, D. P., Wallace, B. A. and Janes, R. W. (2010). 2Struc: the secondary structure server. *Bioinformatics* 26, 2624-2625.
- Kortemme, T. and Creighton, T. E. (1995). Ionisation of cysteine residues at the termini of model α -helical peptides. Relevance to unusual thiol pK a values in proteins of the thioredoxin family. *J Mol Biol* 253, 799-812.
- Li, B., Yang, D., Wang, G., Wang, X., Bai, C. and Dong, C. (2012). Peroxiredoxin 6-Mediated Negative Regulation Of Muc5ac Hyper-Production And Secretion During Asthma. *Am J Respir Crit Care Med* 185, A2763.
- Lill, M. A. and Danielson, M. L. (2011). Computer-aided drug design platform using PyMOL. *J Comput Aided Mol Des* 25, 13-19.
- Lovell, S. C., Davis, I. W., Arendall, W. B., de Bakker, P. I. W., Word, J. M., Prisant, M. G., Richardson, J. S. and Richardson, D. C. (2003). Structure validation by $C\alpha$ geometry: ϕ , ψ and $C\beta$ deviation. *Proteins: Struct., Funct., and Bioinf.* 50, 437-450.
- Maneovich, Y. and Fisher, A. B. (2005). Peroxiredoxin 6, a 1-Cys peroxiredoxin, functions in antioxidant defense and lung phospholipid metabolism. *Free Radic. Biol. Med* 38, 1422-1432.
- Maneovich, Y., Shuvaeva, T., Dodia, C., Kazi, A., Feinstein, S. I. and Fisher, A. B. (2009). Binding of peroxiredoxin 6 to substrate determines differential phospholipid hydroperoxide peroxidase and phospholipase A 2 activities. *Arch. Biochem. Biophys.* 485, 139-149.
- Monteiro, G., Horta, B. B., Pimenta, D. C., Augusto, O. and Netto, L. E. S. (2007). Reduction of 1-Cys peroxiredoxins by ascorbate changes the thiol-specific antioxidant paradigm, revealing another function of vitamin C. *Proc. Natl. Acad. Sci. U.S.A.* 104, 4886-4891.
- Nagy, N., Malik, G., Fisher, A. B. and Das, D. K. (2006). Targeted disruption of peroxiredoxin 6 gene renders the heart vulnerable to ischemia-reperfusion injury. *Am J Physiol Heart Circ Physiol* 291, H2636-H2640.
- Nicolussi, A., D'Inzeo, S., Mincione, G., Buffone, A., Di Marcantonio, M. C., Cotellese, R., Cichella, A., Capalbo, C., Di Gioia, C. and Nardi, F. (2014). PRDX1 and PRDX6 are repressed in papillary thyroid carcinomas via BRAF V600E-dependent and-independent mechanisms. *Int. J. Oncol.* 44, 548-556.
- Pacifici, F., Arriga, R., Sorice, G. P., Capuani, B., Sciolli, M. G., Pastore, D., Donadel, G., Bellia, A., Caratelli, S. and Coppola, A. (2014). Peroxiredoxin 6, a novel player in the pathogenesis of diabetes. *Diabetes* 63, 3210-3220.
- Park, M. H., Jo, M., Kim, Y. R., Lee, C.-K. and Hong, J. T. (2016). Roles of peroxiredoxins in cancer, neurodegenerative diseases and inflammatory diseases. *Pharmacol. ther.* 163, 1-23.
- Peshenko, I. V. and Shichi, H. (2001). Oxidation of active center cysteine of bovine 1-Cys peroxiredoxin to the cysteine sulfenic acid form by peroxide and peroxy nitrite. *Free Radic. Biol. Med* 31, 292-303.
- Rahaman, H., Zhou, S., Dodia, C., Shuvaeva, T., Feinstein, S. I. and Fisher, A. B. (2012). Phosphorylation of Prdx6 mediated by MAP kinase induces conformational change with concomitant increase in its phospholipase A2 activity. *FASEB J.* 26, 997.992-997.992.
- Ralat, L. A., Manevich, Y., Fisher, A. B. and Colman, R. F. (2006). Direct evidence for the formation of a complex between 1-cysteine peroxiredoxin and glutathione S-transferase I• with activity changes in both enzymes. *Biochemistry* 45, 360-372.
- Salmeen, A., Andersen, J. N., Myers, M. P., Meng, T.-C., Hinks, J. A., Tonks, N. K. and Barford, D. (2003). Redox regulation of protein tyrosine phosphatase 1B involves a sulphenyl-amide intermediate. *Nature* 423, 769-773.
- Sharapov, M. G., Ravin, V. K. and Novoselov, V. I. (2014). Peroxiredoxins as multifunctional enzymes. *Mol. Biol.* 48, 520-545.
- Smeets, A., Loumaye, E. o., Clippe, A., Rees, J. F. o., Knoops, B. and Declercq, J. P. (2008). The crystal structure of the C45S mutant of annelid *Arenicola marina* peroxiredoxin 6 supports its assignment to the mechanistically typical 2-Cys subfamily without any formation of toroid-shaped decamers. *Protein Sci.* 17, 700-710.
- Wang, X., Phelan, S. A., Forsman-Semb, K., Taylor, E. F., Petros, C., Brown, A., Lerner, C. P. and Paigen, B. (2003). Mice with targeted mutation of peroxiredoxin 6 develop normally but are susceptible to oxidative stress. *J Biol Chem* 278, 25179-25190.
- Wang, Y., Feinstein, S. I. and Fisher, A. B. (2008). Peroxiredoxin 6 as an antioxidant enzyme: Protection of lung alveolar epithelial type II cells from H₂O₂-induced oxidative stress. *J Cell Biochem* 104, 1274-1285.
- Wiederstein, M. and Sippl, M. J. (2007). ProSA-web: interactive web service for the recognition of errors in three-dimensional structures of proteins. *Nucleic Acids Res* 35, W407-W410.

- Wu, Y.-Z., Manevich, Y., Baldwin, J. L., Dodia, C., Yu, K., Feinstein, S. I. and Fisher, A. B. (2006). Interaction of surfactant protein A with peroxiredoxin 6 regulates phospholipase A2 activity. *J Biol Chem* 281, 7515-7525.
- Wu, Y., Feinstein, S. I., Manevich, Y., Chowdhury, I., Pak, J. H., Kazi, A., Dodia, C., Speicher, D. W. and Fisher, A. B. (2009). Mitogen-activated protein kinase-mediated phosphorylation of peroxiredoxin 6 regulates its phospholipase A2 activity. *Biochem. J* 419, 669-679.
- Yang, J. and Zhang, Y. (2015). Protein Structure and Function Prediction Using I-TASSER. *Curr. prot. Bioinfo.* 52, 5.8.1-5.8.15.
- Yun, H.-M., Choi, D. Y., Oh, K. W. and Hong, J. T. (2015). PRDX6 Exacerbates Dopaminergic Neurodegeneration in a MPTP Mouse Model of Parkinson's Disease. *Mol Neurobiol* 52, 422-431.
- Yun, H.-M., Jin, P., Han, J.-Y., Lee, M.-S., Han, S.-B., Oh, K.-W., Hong, S.-H., Jung, E.-Y. and Hong, J. T. (2013). Acceleration of the development of Alzheimer's disease in amyloid beta-infused peroxiredoxin 6 overexpression transgenic mice. *Mol Neurobiol* 48, 941-951.
- Zhang, Y. (2008). I-TASSER server for protein 3D structure prediction. *BMC Bioinformatics* 9, 1.